

Chapter 3

Fabrication of CSA doped PANi-Ta₂O₅ nanocomposite based chemiresistive thin-film sensor and study of its NO₂ gas sensing behaviour

3.1 Thin film deposition

(Deposition of thin film based on conducting polymer (CP) for gas sensing applications- Methods [20])

Some of the most popular methods employed by the research community to deposit thin films of gas sensing material based on nanostructures of conducting polymers are described below. It is important to consider an appropriate deposition method in order to suit with different sensing material and different configurations of the sensor device. For gas sensing applications, the active layer plays a vital role in the operation of the sensor. An effective control of reproducible thickness of the layer, uniformity and morphological homogeneity at nano-scale level are some of the crucial points to determine the quality of the active layer [97]. These factors are decided by the deposition method to a great extent.

Most of the traditional non-conjugated conducting polymers can be processed in solution form, while conjugated polymers are insoluble in most of the organic solvents due to their stiff conjugation chain.

3.1.1. Electrochemical Deposition or electrodeposition

Electrochemical deposition or electrodeposition is a convenient, well-known method to deposit films of a wide variety of materials including conducting polymers and metals on selected conducting substrates. The film growth process is consisted of the formation of a metallic layer onto a conducting substrate through electrochemical reduction of metal ions from an electrolyte to acquire the desired electrical, corrosion resistance and heat tolerance and to reduce wear and friction. Both positive and negative ions are contained in the electrolyte [114]. To begin the electrodeposition process, the working electrode (cathode) is immersed in the electrolyte contained in the cell along with the counter electrode (anode). Electric current is used for the deposition process. To allow electric current to be flowing along the circuit, the two electrodes are connected to a power source like a battery. The anode

is connected to the positive terminal and the cathode to the negative terminal of the battery and this causes the metal ions to get reduced to metal atoms. This action finally deposits the metallic layer on the substrate. The total charge passed through the electrochemical cell controls the thickness of the film.

Fig. 3.1 shows a schematic of electrodeposition process in an electrolytic cell for depositing a metal (denoted by “M”) from an aqueous solution of metal salt (denoted by “MA”).

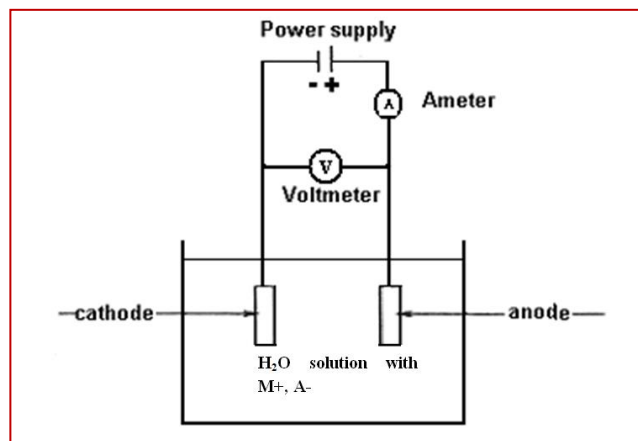


Fig. 3.1. Electrodeposition technique [114].

The film deposition can be carried out on patterned microelectrodes. The electrochemical growth of the thin film is carried out using [galvanostatic](#), [potentiostatic](#) or [voltammetric](#) strategies [115].

In the field of gas sensing, electrochemical deposition of conducting polymers and their derivatives have been used by several past works. Different nanostructures such as nanorods, nanowires, nanotubes, nanoflakes and hybrid nanostructures have been deposited successfully for gas detection using electrochemical synthesis [116], [117]. J. Reemts et al. [118] prepared PANi sensing film in-situ by electrochemical polymerization between two gold electrodes for ethanol and acetone sensing. R. Gangopadhyay et al. [119] performed electropolymerization of pyrrole with cross linked polyvinyl alcohol for ammonia gas

sensing. Fang and co-workers [120] devised micro-gas-sensor for the detection of volatile organic compounds (VOCs) using electrochemically deposited polypyrrole thin film.

The major advantages of electrochemical deposition are cheap, processing capability at room temperature and pressure, less synthetic, simple and eco-friendly. One most attractive feature of this technique is that the deposition thickness, deposition potential and deposition temperature can well be controlled [114]. However, an important limitation, here, is that a non-conducting substrate cannot be used due to the dual role played by the electrode and the substrate [120].

3.1.2. Dip Coating

Dip coating is a convenient and facile approach for thin film deposition and has been used extensively in research purposes. The quality of the deposited film is inconsistent and hence it is not very much suitable for industrial applications. However, dip coating can still be employed at large scale production for fulfilling low standard requirements at a cheaper price, although the method is more suitable for laboratory uses [121].

Dip coating involves immersing a substrate in a bath of solution containing the conducting polymer, removing it to allow for drying or baking in order to form a thin film of the polymer. Dip coating is comprised of the following stages [122], [123].

- **Immersion** - The substrate is immersed in a solution contained in a tank of the coating material at a fixed speed to avoid any vibration affect.
- **Dwelling** - The substrate is kept immersed fully and motionless to allow forming a layer of the coating material on to the substrate.
- **Withdrawal** - The substrate is withdrawn precisely in a controlled manner and at a constant speed to avoid any affects of unwanted vibration. The quicker the substrate is withdrawn from the tank the thicker will be the film formed on the substrate.
- **Drying** - Once fully withdrawn, the liquid starts to evaporate leaving a thin dry film on the surface of the substrate.

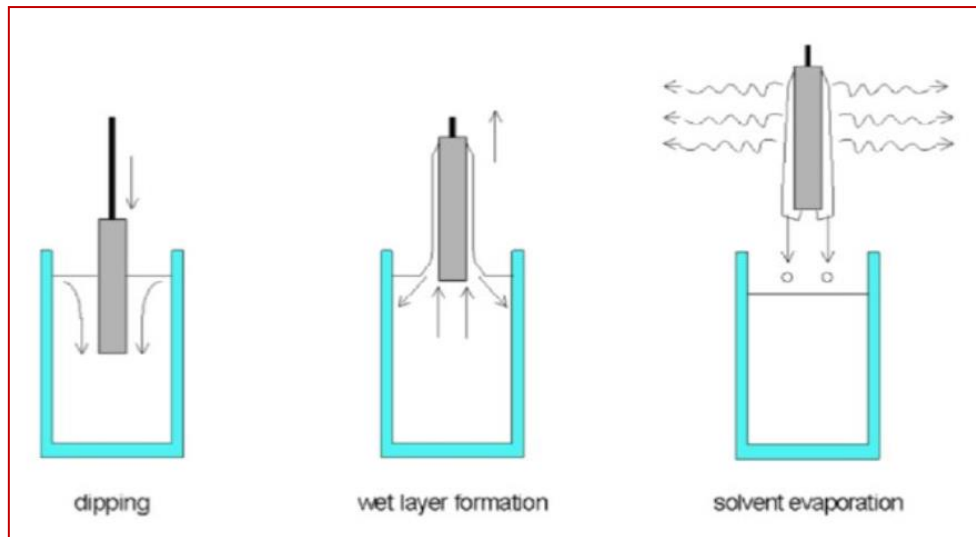


Fig. 3.2. Steps in a dip coating process [124].

For depositing certain materials, an additional stage called **curing** is required. This may cause certain physical or chemical change in the deposited material [124].

Though all the above stages are essential, the withdrawal and drying stages are the most critical ones to determine the quality of the deposited film. The thickness of the film is determined by the complex interplay of entraining forces (to work for retaining the fluid onto the substrate), draining forces (to draw the liquid away from the substrate and back towards the bath) and the drying of the film [123].

In case of depositing a polymer film, some other approaches besides the general technique as discussed above, are also adopted. The substrate is dipped in a solution undergoing chemical polymerization. Accordingly, a part of the polymer is formed as a layer on the substrate. The thickness of the film is usually controlled by the immersion time. Another alternative method is to dip the substrate into the monomer and oxidant solutions. The monomer is polymerized on the surface of the substrate thus forming a layer of the polymer [20].

Y. Yang and his group [125] demonstrated in-situ dip coating polymerization of EDOT monomer to deposit thin layer of poly (3,4-ethylenedioxythiophene (PEDOT) on reduced graphene oxide (RGO) covered substrate using a slow dip coating process. This was a chemiresistor ammonia gas sensor which showed enhanced sensitivity at room temperature. After the baking process, the SEM image of the deposited PEDOT film depicted a porous but

slightly fluctuating morphology. C. Piloto and his group [126] worked on ultrathin carbon nanotube (CNT) sensing film that was produced by surfactant free dip coating dissolved CNTs in chlorosulphonic acid as a working solution for the detection of NO₂ and NH₃ gas at room temperature.

The main advantages of dip coating are its simplicity, adjustable film-thickness and cost effectiveness. The method inhibits the harsh affects of heat, cold, stress and electrical currents. A wide range of film thickness and texture can be obtained. The main disadvantage of this method is its slow speed, non-uniformity of the coating film, and inconsistent quality of the deposited film [127].

3.1.3 Spin-coating

Spin coating is one of the most commonly used techniques of depositing a uniform thin film having thickness ranging from micrometer to nanometer onto a flat substrate. The material to be deposited is dissolved in a solvent. The solution is subsequently spread over a rotating substrate. The substrate is mounted on a rotating chuck and spun at a high speed. A centrifugal force develops there which drives the liquid radially outward [128]. The thickness of the deposited film is determined by the spinning speed, surface tension and viscosity of the solution. The solvent gets evaporated partly during the spinning speed and partly by subsequent drying at an elevated temperature. A solid, smooth film is finally formed on the substrate [129].

Spin coating is extensively used for depositing conducting polymer film on a conducting or non-conducting substrate. The conducting polymer is either dissolved or dispersed in a suitable organic or inorganic solvent. The process can be repeated to obtain the desired thickness of the film. The concentration of the solution and the rate of rotation can be important factors for adjusting the film thickness [20].

As shown in Fig.3.3, spin coating can be consisted of four different stages taking place sequentially viz., fluid-dispense (deposition), spin up, spin off and evaporation. The advantage of spin coating is that a very uniform, thin coating can be obtained, but this method is difficult to apply on large area substrate. As the size of the substrate increases, the high-speed spinning becomes difficult to apply. Also, the material utilization is very non-efficient. In

general, 95%-98% of the sample material is wasted and disposed off during the spin-in process and only 2%-5% of the material gets dispensed on the substrate [130].

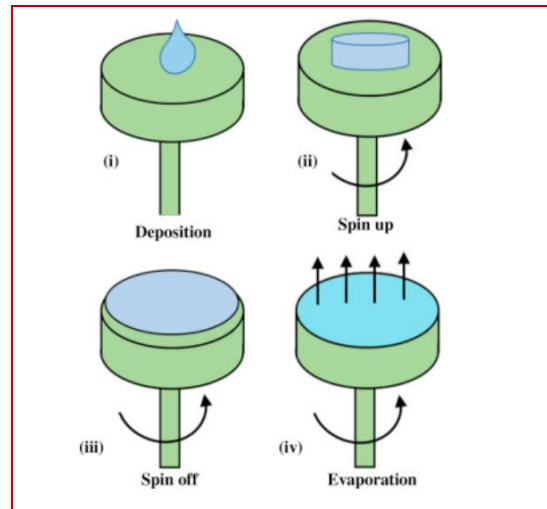


Fig. 3.3. Various stages of spin coating [130].

3.1.4. Langmuir-Blodgett technique

Langmuir-Blodgett (LB) technique is one of the most promising methods for the formation of thin film as it delivers the following features.

- The monolayer thickness can be controlled precisely.
- The monolayer can be deposited homogeneously over large area.
- Multilayer components with varying layer composition can be prepared.
- Monolayers can be deposited on almost any kind of substrates.

A Langmuir monolayer is the one with one molecule thickness that forms at the interface of air and water. To form this layer, the surfactant (surface-active agent) must be insoluble in water. Irvine Langmuir received Nobel prize in Chemistry in 1932 for his investigation on the monolayers which are named after him. The Langmuir monolayer consists of amphiphilic molecules with a hydrophilic (water soluble – polar) head group and a hydrophobic (water insoluble – nonpolar) tail group. The hydrophobic section sits just under the water surface and the hydrophilic section just above the water surface into the air [131], [132].

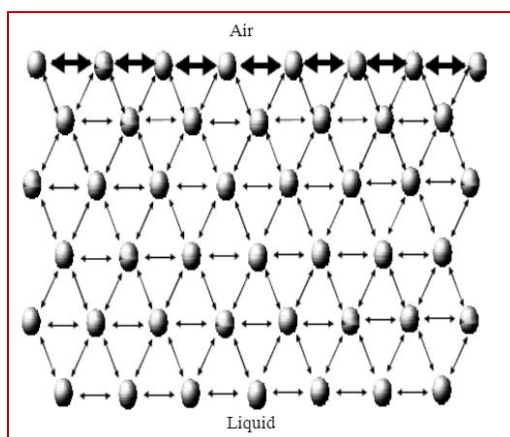


Fig. 3.4. Molecule interaction at air-water interface [133].

The molecular interaction at the interface of air and water- a polar liquid is illustrated in Fig. 3.4. The LB method requires the material to be deposited on the substrate insoluble in water (hydrophobic). Amphiphiles are the molecules consisted of a “head” group of hydrophilic (water soluble) and a “tail” group of hydrophobic compounds. The tail regions are comprised of saturated or unsaturated hydrocarbon chains [133]. Fig. 3.5 illustrates the components and orientation of an amphiphile molecule formed at the interface leading to the formation of an LB monolayer on the water surface as shown in Fig. 3.6. Formation of a stable monolayer of hydrophobic material is the first step in the LB deposition technique [134].

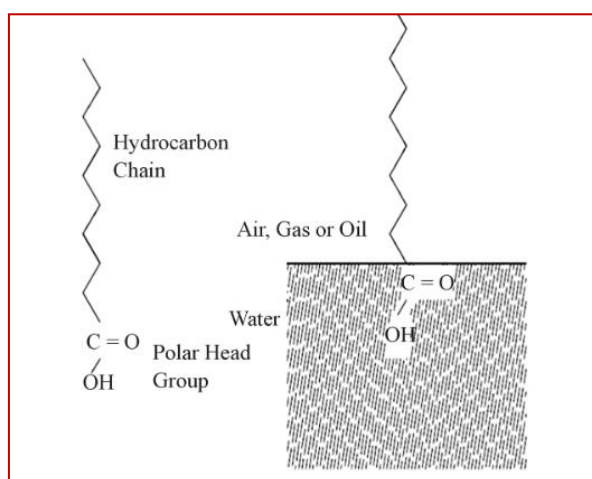


Fig. 3.5. Components and orientation of an amphiphile molecule formed at the interface [133].

A LB film is a nanostructure formed when Langmuir monolayer (of water-insoluble organic particles) is transferred from the air-water interface to solid support by vertical dipping of a flat substrate immersed in the aqueous subphase. The substrate is then extracted in a

controlled way with the adsorbed film onto it. This method is employed to form thin films of conducting polymers, quantum dots and silver nanowires [134].

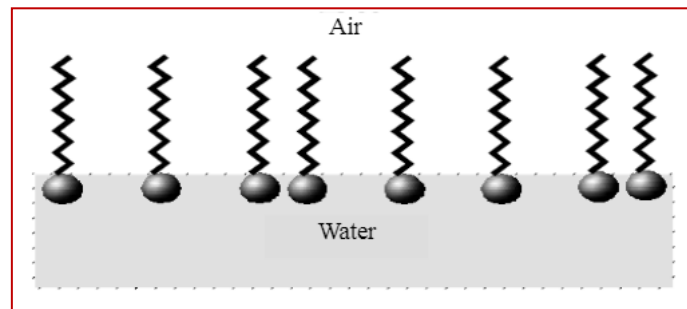


Fig. 3.6. Langmuir monolayer spread on the water surface [133].

N.E. Agbor et al. [135] devised an optical gas sensor based on Langmuir-Blodgett film of PANi using surface plasmon resonance. The sensor exhibited response to both NO_2 and H_2S with reversibility and low detection limit. S. Choudhury et al. [136] demonstrated a room temperature operated hydrogen gas sensor based on PdO (Palladium oxide) nanoparticle based thin film deposited by Langmuir-Blodgett technique. This PdO film was devised as chemiresistive sensor which showed H_2 gas sensitivity in the range of 30-4000 ppm at room temperature.

For gas sensing applications, it is crucial to control the molecular structure of the sensing material for better results. The LB technique enables an effective control of the molecular structure. As the thickness of the sensing layer is decreased, the gas sensitivity increases and vice-versa [133]. More efforts are needed to obtain improved homogeneous films which may otherwise be affected by poor molecular alignment. LB technique suffers from some inherent drawbacks such as poor thermal stability and difficulty in mass production. For applying this method in real applications, the trough design needs to be changed drastically, miniaturized and conveniently be linked with other industrial units [137].

3.1.5. Thermal Evaporation

Thermal evaporation is one of the versatile techniques of physical vapour deposition of thin film which uses vacuum technology for applying coatings of pure materials on various kinds of substrates such as semiconductor wafers, solar cells, optical components and many others. This process was first devised by Faraday in 1850s. The deposited film can have thickness

ranging from nanometers to micrometers [138]. The various components of a thermal evaporation process and schematic of the process are shown in Fig. 3.7 and 3.8.

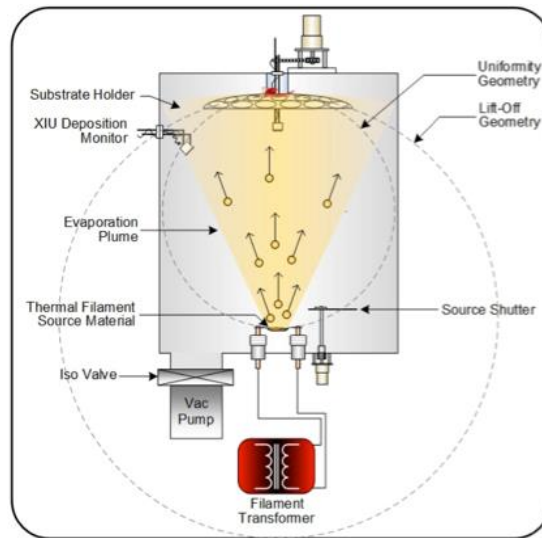


Fig.3.7. Components of a thermal evaporation system [138].

In thermal evaporation process, the bulk material (target) to be deposited is placed in a metal crucible inside a controlled vacuum chamber. The crucible is heated either by resistively passing electric current or by a heater filament. The solid material is heated by Joule effect to an appropriate temperature, producing appreciable vapour pressure. Inside the chamber, even a relatively low vapour pressure is sufficient to create a vapour cloud. This vapour flux of the evaporated material traverses the chamber and forms a film on the substrate. In most cases of this deposition process, the material to be deposited is heated to melting point and the liquid form is kept at the bottom of the chamber, often in an upright crucible. The vapour then rises up towards the top of the chamber where the substrate is held inverted in appropriate fixtures. The substrate thus faces down toward the heated material to receive the coating [139]. The process of thermal evaporation is illustrated in Fig. 3.8.

M.B. Rahmani et al. [140] thermally evaporated molybdenum trioxide (MoO_3) on quartz substrate with gold interdigital fingers for NO_2 and H_2 gas sensing. It was revealed that these evaporative techniques can ensure highly crystalline and layered structure of the deposited material which can possess improved gas sensitivity. A. Kaushik et al. [74] fabricated cross-

linked thin film of PANi and tungsten trioxide (WO_3) using vacuum thermal evaporation for the detection of NO_x gas at room temperature.

Major advantages of thermal evaporation are its relative simplicity, high deposition rate and low contamination of the deposited film (due to low pressure). Highly pure films are good for Schottky contacts [140]. High adhesion between the thin film and the substrate can be achieved. Chemical interaction between the charge and the crucible can take place. This method is not suitable for fabricating multiple-component thin film as some bulk material may evaporate before others due to their differences in melting points and vapour pressures [139].

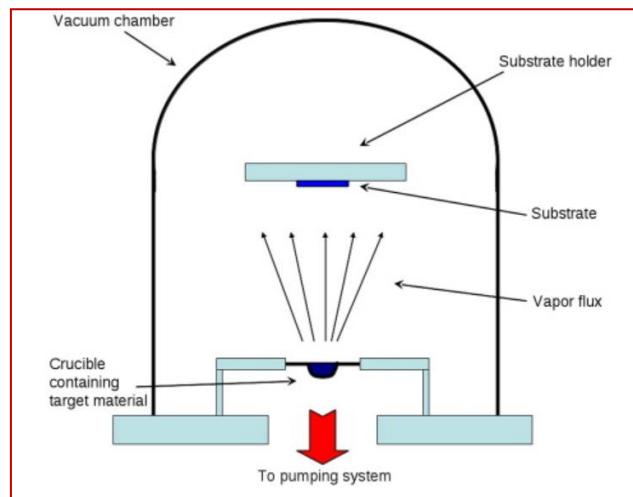


Fig.3.8. Schematic representation of thermal evaporation process [139].

3.2 Chemiresistive Gas Sensors and their Gas Sensing Mechanism

3.2.1 Chemiresistors– operation and structure

In modern days, gas sensors find their wide applications in the fields of public security, domestic safety, monitoring industrial toxic gas emission, underground mining, environment and health. Different types of gas sensors, such as, [chemiresistive](#), [electrochemical](#), [optical](#), [surface acoustic wave](#) are being used in different areas for the detection of combustible, explosive, environmentally toxic gases and the VOCs. Among them, chemiresistive gas

sensors have gained popularity owing to their facile structure, low cost, simple fabrication and operation, and ease of highly precise measurements [141], [142].

Depending on the sensor type, there is change in physical conditions or chemical composition of the sensing material, such as permeability, resistance (or conductivity), capacitance, temperature, acoustic wave, resulting from the interaction of the target gas and the surface atoms (O^- , O^{2-} , H^+ , OH^-) by adsorption or desorption of gas molecules at a particular operating temperature. The sensor produces signals which can be correlated to the concentration of the target gas [143].

A chemiresistor is a class of chemical sensors that changes its electrical resistance under the influence of a change in the nearby chemical environment. The device relies on a direct chemical interaction between the sensing material and the analyte. This chemical interaction can be based on covalent bonding, hydrogen bonding, metal coordination, hydrophobic forces, van der Waals forces, π - π interactions, halogen bonding, electrostatic and electromagnetic effects. The sensor is the most important component built inside a portable or fixed device, which emits an alarm in the form of sound or signal when the measured gas exceeds the threshold value. The sensor device can determine several gas sensing parameters. Among these, sensor response, selectivity, stability and response time are the most important ones. Apart from them, recovery time, reproducibility and power consumption are also some significant parameters [144].

The chemiresistive sensor exhibits a change in resistance on exposure to a target gas. Electrical resistance is the simple electrical signal that can be easily analyzed requiring minimum supporting electronics for building compact, self-contained sensor device [145].

A basic chemiresistor comprises of a sensing material that bridges the space between two electrodes as shown in Fig.3.9.a. The electrodes are also commonly fabricated as interdigitated structure as shown in Fig.3.9.b. The interdigitated configuration maximizes the contact area between the electrodes, the sensing material and the analyte [146].

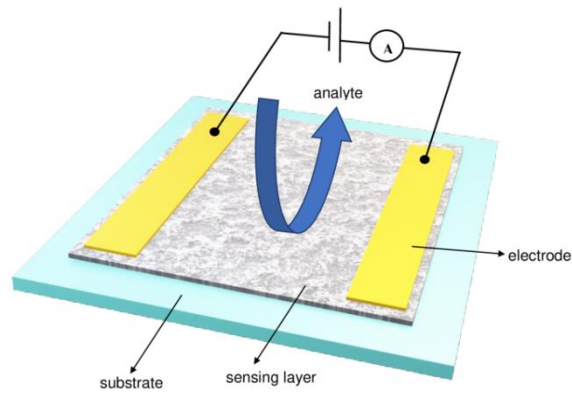


Fig. 3.9.a. Schematic of chemiresistive thin-film gas sensors with two electrodes.

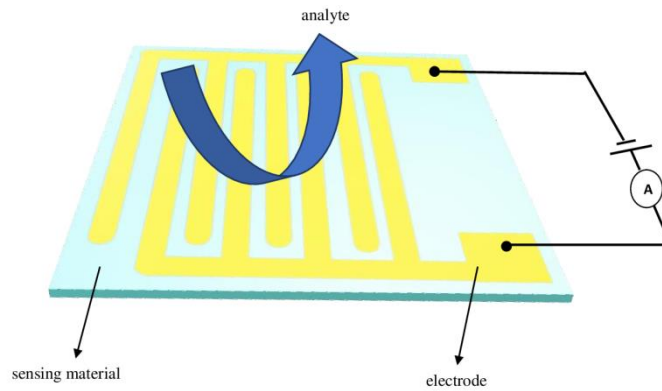


Fig. 3.9.b. Use of interdigitated electrode in chemiresistive thin-film gas sensor.

The layer of the sensing material is also called the active layer. The resistance between the electrodes built in contact with the active layer can easily be measured. The sensing material has a default resistance that changes with the presence or absence of the analyte. During exposure, the analyte comes into contact with the sensing material, causing change in the resistance of the later. The change in resistance can indicate the presence of the analyte gas and also in many cases, the amount and type of the analyte. With the increase or decrease of the analyte level, the change in resistance varies. The change in resistance is from a baseline level (say, R_{air}) to a steady level of resistance when exposed to the analyte gas (say, R_{gas}) on removing the gas inflow. This gives a measure of sensor response [145][147]. The surface area, structural morphology, chemical composition and sensing temperature play vital role in influencing the sensor response [142].

As revealed by several past research works, the chemiresistive properties can be exhibited by different materials such as [nanostructured metal-oxide semiconductors \(MOS\)](#), [conducting polymers \(CPs\)](#), [advanced nanomaterials like graphene, carbon nanotubes, gold nanoparticles](#) [146].

3.2.1.1 MOS based gas sensors

Chemiresistive gas sensors based on semiconductor metal-oxide (MOS) nanostructures have been successfully implemented with promising results.

Semiconducting metal oxides such as [ZnO](#), [SnO₂](#), [TiO₂](#), [Ta₂O₅](#), [WO₃](#) are wide band gap semiconductors and they respond to surrounding gas concentration with proportional change in electrical conductivity. Increasing the surface-to-volume ratio is one of the attractive options to enhance the performance of these sensors. Till recently a good no. of 1D/2D/3D semiconductor metal oxide nanostructures have been developed that revolutionised the gas sensing arena. Nanostructures such as nanowires, nanobelts [148], nanorods [149], [150], nanoflowers [151], nanospheres [152], [153], nanobricks [154] and nanoprisms [155] have been effectively applied in gas sensors to achieve excellent performance.

Duoc et al. [150] synthesized on-chip ZnO nanorods and nanowires using hydrothermal method for room temperature NO₂ gas detection. It was found that nanowires were more sensitive to the gas than nanorods. N.D. Dien et al. [156] synthesized one-dimensional, self-assembled, single-crystal hexagonal WO₃ nanorods by hydrothermal processing and fabricated the material on SiO₂/Si substrate with platinum interdigitated electrodes. High sensitivity and selectivity to NH₃ were achieved by the sensor at low operating temperature of 50⁰C. W. Zeng et al. [157] reported the synthesis of hierarchical nanospheres of SnO₂ decorating TiO₂ nanobelts for detecting VOCs of different species. The improved gas sensing feature was attributed to the enhanced electron transfer between the SnO₂ nanospheres and the adsorbed oxygen species as well as to the heterojunctions of the SnO₂ nanospheres to the TiO₂ nanobelts. Synthesis of crystalline ZnO nanorods and prisms through continuous hydrothermal flow is reported by L. Shi et al. [155] that showed excellent NO₂ gas sensitivity. Continuous hydrothermal flow synthesis of crystalline ZnO nanorods and prisms is reported via a new pilot-scale continuous hydrothermal reactor (at nominal production rates of up to 1.2 gm/hour). Different size and shape particles of ZnO (wurtzite structure) were

obtained via altering reaction conditions such as the concentration of either additive H₂O₂ or metal salt. Selected ZnO samples (used as prepared) were evaluated as solid oxide gas sensors, showing excellent sensitivity toward NO₂ gas. It was found that both the working temperature and gas concentration significantly affected the NO₂ gas response at concentrations as low as 1 ppm.

M. Yang et al. [158] devised a holey graphene-oxide based chemiresistive thin film sensor for detecting ammonia (NH₃) gas. The device showed excellent response and selectivity to NH₃. The resistance change was recorded at 2.81% at 1 ppm NH₃, while the resistance change was 11.32% when the NH₃ concentration was increased to 50 ppm. S. Kumar et al. [159] fabricated a chemiresistive thin-film sensor based on polyethylenimine (PEI) functionalized single-walled carbon nanotube which detected NO₂ gas. The sensor showed a sensitivity of 20.12% towards 20 ppm gas which increased substantially to 37% towards 50 ppm gas.

Though a large no. of MOS based gas sensors have been reported with excellent gas sensing properties, there still lies several challenges that hinder the performance of these sensors. The environmental humidity is one of the adverse factors which can deteriorate the sensitivity to a great extent [160]. On exposure to humidity, increase/decrease in the bands of metal-oxide lattice bonds and formation of hydroxyl groups take place [161]. Issues like high operating temperature, poor selectivity and low stability are some of the important concerns of the MOS based gas sensors to be addressed [143].

Although researchers have devoted noteworthy efforts to improve the sensing material, there is still room for further improving the performance of the MOS based sensors, increasing their reliability and robustness for practical applications. It is anticipated that development of novel nanostructures/nanocomposites, incorporation of porous nanostructures can lead to gas sensors with improved sensitivity, high response and recovery aspects [162].

3.2.1.2 CP based gas sensors

As discussed earlier, CP based gas sensors are poised with diverse portfolio of inherent advantages such as controllable morphology of the sensing material, structural flexibility, easy fabrication techniques, cost-effectiveness, room-temperature operability [27].

The current work aims at studying gas sensors based on CPs. So, focus is made on this class of sensing device in the subsequent discussions.

A vast no. of chemiresistive thin-film gas sensors based on CPs has been reported in the past with encouraging results. Some of them are discussed in the earlier chapter. Chem-resistive gas sensors based on CP based hybrid materials are bestowed with high response and selectivity, short response/recovery time, good repeatability and stability, easy processing and low operating temperature [17]. Because of room temperature operability, the additional heating arrangement is not needed which leads to low processing cost and easy mass production.

The operation of these sensors can be greatly altered by nanostructuring, doping and adding inorganic materials. The resulting sensor output exploits charge transport of the primary charge carrier and adsorption/desorption of the target gas. The sensor performance is characterized by several important parameters such as response, selectivity, response time, recovery time, operating temperature, life-time and limit of detection. Resistance/conductivity change is the primary measurement for determining the sensor response [144].

Conducting polymers such as polyaniline (PANi), polypyrrole (Ppy), polythiophene (PTh), polyacetylene (PA) and poly(3,4ethylenedioxythiophene) (PEDOT) have been found as some of the most suitable materials for gas sensing at room temperature. Several works witnessed promising results from CP based sensors in terms of sensing response compared to semiconducting metal oxide based sensors.

Sharma et al. [45] devised 1% PANi doped SnO₂ sensor that showed response of 3.01×10^2 towards 10 ppm of NO₂ gas at 40⁰C. Earlier the same group fabricated SnO₂ thin film which exhibited high sensor response of $\sim 2.9 \times 10^4$ towards 100 ppm of NO₂ gas at 100⁰C. N. Gaikwad et al. [163] devised LPG sensors based on Platinum/Ppy nanocomposite which showed excellent gas sensitivity at relatively low temperature. H.K. Khorami et al. [164] reported room-temperature operated ammonia gas sensors based on hybrid SnO₂-ZnO/Ppy nanocomposite to achieve highly improved gas sensing features.

Metal oxide based sensors can exhibit promising results due to alteration of oxygen stoichiometry and electrically active surface charges, but at the cost of high operating temperature (150⁰C-400⁰C) [165]. High operating temperature induces gradual change in the properties of the nanostructures and causes fusion of grain boundaries, thus reducing stability and life-term of the device [76].

The shortcomings of CPs, such as low conductivity and poor stability, and of inorganic metal oxides, such as the need for operation at high-temperature and sophisticated processing requirement make them inapt for gas sensor fabrication. In this scenario, the use of a nanocomposite composed of these two types of materials may facilitate effective gas sensing traits and allow the sensor to be functional at low temperature [76].

3.2.2 Gas sensing mechanism

The type of the deposition technique of the sensing layer as discussed above, can influence several important surface properties such as morphology, surface defects, grain boundaries, porosity etc. Also the kind of the target gas, reducing or oxidizing and p-type or n-type of the sensing material significantly determines the sensor performance. The adsorbed oxygen species in the atmosphere also plays an important role in determining the gas sensing properties.

3.2.2.1 Role of adsorbed oxygen species in gas sensing

One major role is played by the oxygen atoms adsorbed at the sensing surface. It is established by earlier studies that in case of most semiconductor based metal oxide sensors, adsorbed oxygen offers a significant in the sensing mechanism. Different oxygen species are determined by the working temperature and grain size [166], [167], [168].

The adsorbed oxygen species are regarded as free electrostatically stabilized oxygen ions with no local chemical bond. The adsorption reaction takes place at the sensing surface and it depends on the type of the analyte gas. Atmospheric oxygen (O₂) forms different oxygen species (O⁻ -- oxygen ion, O²⁻ -- superoxide anion, O₂⁻ -- peroxide ion) which depend on working temperature [169]. The oxygen chemisorptions follow the process as described in equations 3.1 through 3.4 [168].



The adsorbed oxygen species have been regarded as free oxygen ions electrostatically stabilized on the surface (with no local chemical bond formation). Peroxide and superoxide are oxides containing oxygen atoms. The main difference between peroxide and superoxide is that the oxidation state of oxygen in peroxide is -1 whereas the oxidation state of oxygen in superoxide is -1/2 [169].

Apart from the adsorbed oxygen species, the lattice oxygen and interstitial oxygen atoms also play vital role in the gas sensing process. The lattice of an oxide can act as reservoir for oxygen, storing and releasing them under suitable conditions [170]. An interstitial ion of a foreign atom may migrate into a vacant lattice site of the host material. An interstitial site appears when a particle is missing from the lattice. These situations are called as interstitial defects as shown in Fig. 3.10 [171], [172]. These are further discussed in the following sections.

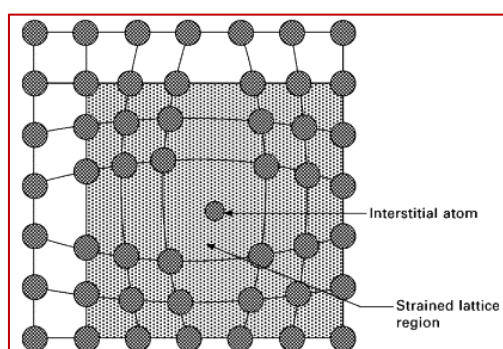


Fig. 3.10. Interstitial defects [172].

3.2.2.2 Interaction of the analyte gas and the conducting polymer

The physical properties of the CPs can be changed by doping or dedoping. The doping levels of the CPs are changed when they come in contact with analyte gas at room temperature.

When the CPs are exposed to the analyte gas, electron transfer takes place and hence change in resistance and work function of the sensing material take place. Work function is defined as the minimum energy needed by an electron to escape the metal surface and move to the vacuum energy level. This phenomenon can be noticed when the CPs like PANi, Ppy, PTh comes in contact with redox-active gases like NH₃, NO₂, H₂S, I₂ [20]. Oxidation-reduction (redox) reactions cause the transfer of electrons between chemical entities. Oxidation involves in the loss of electrons or the increase of the oxidation states by a molecule. The electrons lost by a molecule during oxidation process are accepted by another molecule that gets reduced in the process [173].

Oxidizing or electron-accepting gases like NO₂, CO₂, I₂ can remove electrons from the aromatic rings of the CPs. When this happens with p-type CPs like PANi, Ppy etc. the doping level and the electrical conductivity of the CP gets increased. The opposite scenario is seen in case of reducing or electron-donating gases like NH₃, H₂S. Equations 3.5 and 3.6 are the possible reactions when Ppy is exposed to NH₃ [20].



As shown in above expressions, Ppy is positively charged in oxidized state (Ppy⁺) and neutral in the reduced state (Ppy⁰).

In case of PANi, the doping state of PANi can be controlled by exposing it to acid/base gases. When exposed to reducing gas NH₃ (acting as a base), it undergoes dedoping by deprotonation. The protons on –NH group of PANi transferred to NH₃ molecules to form NH₄⁺ while PANi itself changes into base form. This process is reversible. When NH₃ gas is removed, NH₄⁺ ions can be decomposed to ammonia gas and proton. On the other hand, with the loss of H⁺, the electron-hole concentration of PANi becomes low. Hence the resistance of the sensor increases. When the sensor is exposed to air by removing NH₃, PANi takes H⁺ from NH₄⁺, the electron-hole concentration of PANi recovers. The resistance decreases to the initial value [20].

When exposed to acidic gases like NO_2 , H_2S , HCl , CO_2 in water, PANi will be doped. PANi when exposed to oxidizing gas NO_2 (electron acceptor), the reaction mechanism as shown in Fig.3.11 may possibly take place. The stable resonance structure of NO_2 is $\text{O}=\text{N}^+-\text{O}^-$ with the nitrogen atom having a positive charge and an unpaired electron. This nitrogen atom will withdraw an electron from the $-\text{NH}$ group. The positive charge at the nitrogen atom is transferred to the amine group, causing a net increase in positive charge in the PANi backbone and hence an increase in conductivity.

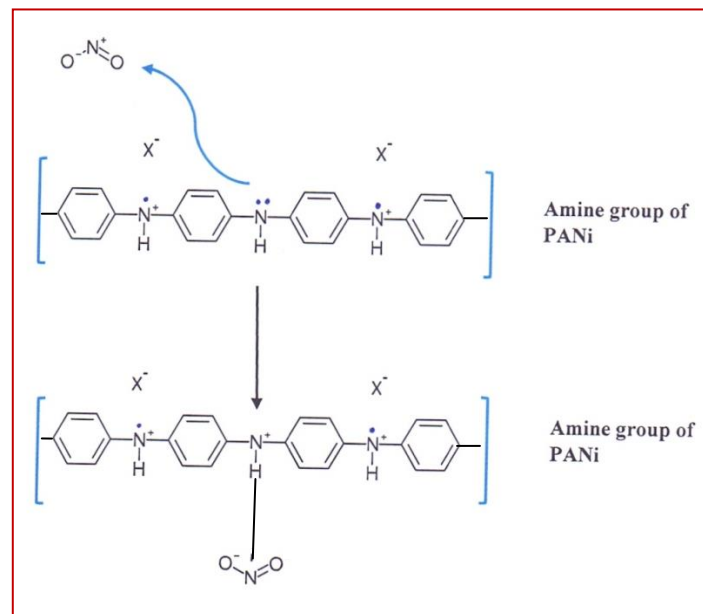


Fig. 3.11. Possible reaction mechanism between PANi and NO_2 .

NH_3 as a strong reducing agent results in lowering the conductivity due to the elimination of free hole charge carriers in the sensing layer, while NO_2 increases the conductivity due to the generation of additional free hole charge carriers [174].

3.2.3. Gas sensing characteristics [177], [178]

In the literature, a number of basic gas sensing parameters are reported for gas sensors. They are [sensor response](#) or [gas sensitivity](#), [selectivity](#), [reproducibility](#), [response time](#), [recovery time](#), [operating temperature](#), [analyte concentration](#), [life-time](#), [stability](#) and [detection limit](#).

a) Sensor Response (S)

No uniform definition of sensor response is found in the literature. More commonly sensor response is defined as the ratio of sensor's resistance in the presence of the analyte gas (R_g) to that in the reference gas (R_a), i.e, R_g/R_a . The reference gas is usually air or an inert gas such as dry nitrogen gas. In case of p-type material towards oxidizing gas it is R_g/R_a and R_a/R_g towards reducing gas. This becomes vice-versa for n-type materials.

Different mathematical expressions are used for sensor response (p-type) towards oxidizing gas (for $R_g < R_a$) by different groups of researchers as given below in equations 3.7 through 3.9.

$$S = \frac{R_g}{R_a} \quad [179] \quad (3.7)$$

$$S = \frac{R_a - R_g}{R_a} \quad [180] \quad (3.8)$$

$$S = \frac{R_a - R_g}{R_a} \times 100\% = \frac{\Delta R}{R_a} \times 100\% \quad [181] \quad (3.9)$$

Table- 3.1.a

(Summary of sensor response for different types of sensing material and target gas) [146], [182]

Type of sensor	Type of analyte (target gas)	Primary charge carrier	Sensor response
p-type	Oxidizing	Holes	resistance decreases
p-type	Reducing	Holes	resistance increases
n-type	Oxidizing	Electrons	resistance increases
n-type	Reducing	Electrons	resistance decreases

Table- 3.1.b [146]

(Examples of oxidizing and reducing analytes)

Examples of oxidizing analytes	Examples of reducing analytes
NO _x , CO ₂ , SO ₂ , O ₂ , O ₃	NH ₃ , CO, CH ₄ , H ₂ , H ₂ S, acetone, ethanol, methanol

The sensing response behaviour of p-type and n-type sensors towards different oxidizing and reducing gases are summarised in table 3.1.a The various oxidizing and reducing gases researched commonly for detection are shown in table 3.1.b.

b) Response time and recovery time

Response time is generally defined as the time taken for a material's resistance to reach 90% of the total response during its exposure to the analyte. On the contrast, recovery time is defined as the time taken to return to 90% of the original steady-state resistance value on removal of the analyte.

c) Selectivity

Selectivity is the ability of the sensor how well it responds to a particular analyte gas in the presence of a no. of other gases. A good sensor can significantly discriminate a particular gas in a mixture of several gases.

d) Stability

Stability is the ability of a sensor to produce reproducible results over a certain period of time. The characteristics of sensor time, selectivity, response and recovery time must be retained during this period of time.

e) Reproducibility or repeatability

Reproducibility or repeatability is the ability of the sensor to exhibit stability and same results under the similar measuring conditions over repeated cycles.

f) Operating temperature

The temperature at which the sensor can function to give measurable response is the operating temperature. The operating temperature of many metal oxide based sensors is high (>200°C). As an example, some SnO₂ based sensors operate at 400°C, when free electrons

flow through the grain boundaries of the SnO₂ crystals. But not all sensors operate at high temperature. The response of ZnO to oxygen is ambient temperature, but it is high temperature of about 400⁰C to hydrogen. Many good sensors operate at room temperature. The type of the sensing material and its growth process, sensor geometry, the kind of gas to detect are some of the parameters that play a key role in reducing the operating temperature of the sensor.

g) Detection limit

Detection limit is the minimum concentration of the analyte that can be detected by the sensor under given conditions and at a particular temperature.

h) Life time

Life time of a sensor is the time period over which it can continuously operate without performance degradation.

For an ideal chemical sensor, it is desired to have essentially high response, good selectivity with fast response and recovery time and low operating temperature. In applications, it is important that the sensor provides high precision and sensing capability for large number of cycles without hysteresis. The sensor should exhibit invulnerability towards adverse effects of humidity, temperature, acids, alkalis, dust and vibrations. Besides all these desirable factors, the sensing material should be robust, safe, non toxic with long life-time and non-complex operation. These criteria designate a sensor device suitable for a practical application [178].

Investigators usually make attempt to achieve some of the above mentioned ideal characteristics, overlooking the others. It is rather elusive to create an ideal sensor. Real applications do not require sensors with all desirable characteristics to be fulfilled. For example, in an industrial application monitoring a particular concentration of a gas, ppb level detection limit is not important but response time in seconds may be highly required. On the other hand, in case of environmental monitoring, lower detection limit of the pollutant gas may be of utmost importance, but a response time of fewer seconds is acceptable [182].

3.3. Experimental– Fabrication of CSA doped PANi-Ta₂O₅ based NO₂ gas sensor

3.3.1 Fabrication of PANi-Ta₂O₅-CSA based chemiresistive thin film sensor

PANi in EB form was taken in fine powdered form and is grinded with Ta₂O₅. Then this mixture was grinded with CSA (solid). All these materials were taken in right proportion as given in table 2.1 and grinded in a mortar for 1 hour to get the following samples for subsequent thin film preparation, viz., PANi-Ta₂O₅(50wt%), PANi-Ta₂O₅-CSA20%, PANi-Ta₂O₅-CSA30% and PANi-Ta₂O₅-CSA40% (to refer table 2.1.b) . Each of these powdered samples including pure PANi-EB was dispersed in NMP (N-methylpyrrolidone) such that the proportion was 0.5 gm of sample in 20 ml of NMP. Each of the dispersions was kept on stirring for 4 hours. The fabrication steps of the thin film sensor are illustrated in figure 3.12.

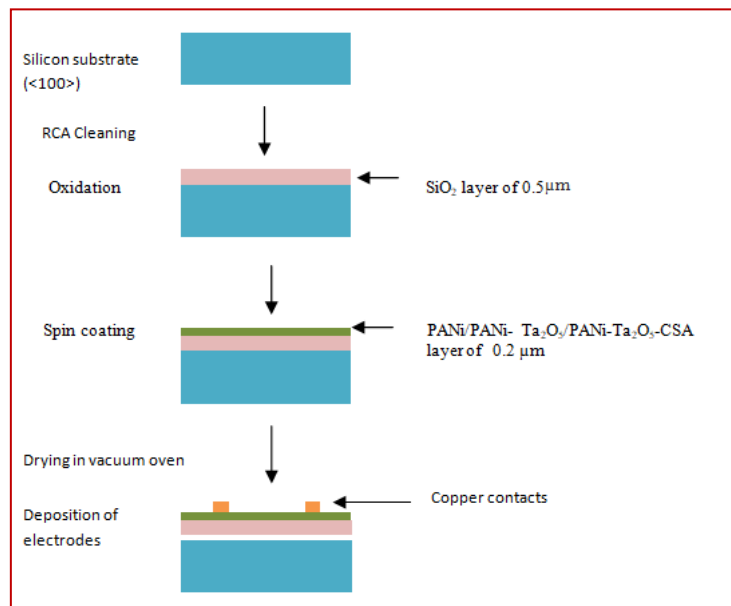


Fig.3.12. Fabrication steps in the preparation of the PANi-Ta₂O₅-CSA based thin-film sensor [75].

Silicon substrate of dimension 1.5 cm × 1 cm was used to make the thin film sensor. To begin with, the substrate was thoroughly cleaned using RCA-1 and RCA-2. After cleaning and blow drying at room temperature, the insulating layer of SiO₂ of 0.5μm thickness was deposited. This polymer solution was spin coated on the silicon substrate at 800 rpm for 60

seconds. Uniform layer of PANi/PANi-Ta₂O₅/PANi-Ta₂O₅-CSA of thickness of 0.2 μm thus formed on the substrate. Next, the substrate was withdrawn and made to dry at vacuum oven for 1 hour. Copper contacts of 0.5 mm width were then deposited using metallization to make the electrodes. The schematic of the thin film sensor device is shown in figure 3.13.

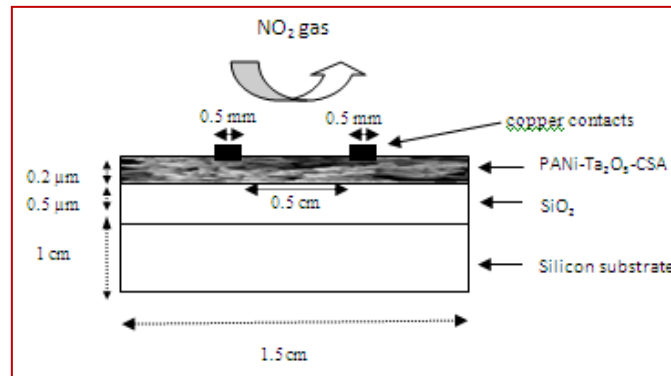


Fig. 3.13. Schematic of the thin-film sensor for NO₂ gas sensing [75].

3.3.2 The gas sensing setup

An in-house gas sensing set-up was used for making the gas sensing measurements. The schematic and the photographs of the gas sensing setup are shown in Fig. 3.14 and 3.15 respectively. All the measurements were carried out at room temperature and relative humidity 60% RH. The gas sensing unit was connected to a Keithly 2100 6½ digital multimeter. The thin film sample was mounted in a glass chamber of volume 200 ml. A fixed voltage was applied to the sample until a steady current value was observed. Nitrogen gas was used as the carrier gas. NO₂ gas was taken from a calibrated cylinder of 100 ppm, diluted in nitrogen and injected at different concentrations to record the change in resistance. The gas flow rates were adjusted using mass flow controllers (MFC). Prior to every set of measurement, the sample was placed inside the chamber for 30 minutes in an ambience of N₂ gas (200 ml/min.) for stability. The resistance changes in the sensor device (R_g and R_a) were obtained by simple calculations, where R_g and R_a are the resistances of the sensing device after and before the exposure to the NO₂ gas.

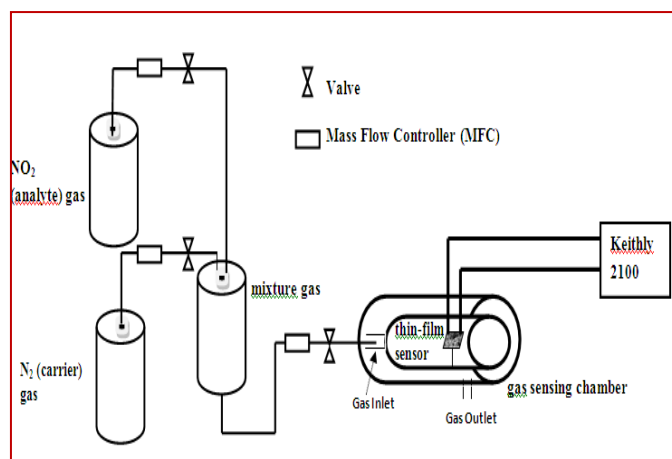


Fig. 3.14. Schematic of in-house gas sensing setup for NO_2 gas sensing [75].



Fig.3.15. Photographs of experimental setup used for gas sensing [courtesy – gas sensing unit, Tezpur University].

3.4 Results and discussion

3.4.1 Gas Sensing mechanism of CSA doped PANi- Ta_2O_5 nanocomposite towards NO_2

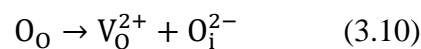
The possible interaction of PANi and NO_2 gas is discussed in the earlier section. It is emerged that NO_2 can play an effective role in enhancing conductivity of the polymer. NO_2 acts as the electron accepting analyte which on contact with the π -electron cloud of

polyaniline, takes electrons from it. When this happens, the polymer becomes positively charged with holes. The charge carriers thus created give rise to the increased conductivity of the sensing film.

To have an insight of the part played by Ta₂O₅ in the gas sensing process, it can be stated that Ta₂O₅ is attached to the PANi molecule through some weak intermolecular bond like van der Waals force forming the PANi-Ta₂O₅ nanocomposite. These weak van der Waals interactions allow the NO₂ gas molecules to infiltrate easily into the polymer matrix. This is further discussed in the following section.

The role played by Ta₂O₅ in the gas sensing mechanism reveals an interesting picture. The oxide carries a larger population of lattice oxygen (O_O or O²⁻) than adsorbed oxygen (O_{ads}). Here, not the adsorbed oxygen but the lattice oxygen of Ta₂O₅ involved in the gas sensing mechanism [176], [181]. It is also shown that excess oxygen in the form of small and mobile interstitial oxygen anions [182] in the lattice can contribute to an increase in p-type conductivity [155]. The generation of interstitial oxygen atoms from the surface oxygen vacancies can be demonstrated according to equation 3.10.

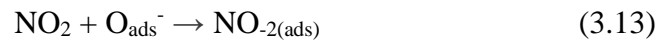
During solid-state doping of PANi with Ta₂O₅ and CSA, thermal vibrations may result in the formation of interstitial oxygen atoms which leave their original Ta₂O₅ crystal site and move to a nearby interstitial site [44]. Following the Kroger-Vink notation, we can write the following expressions.



Here, O_i is the interstitial oxygen, V_O the positively charged vacancies on oxygen sites and O_O is the lattice oxygen in the form of regular occupied oxygen or the lattice oxygen anion (O²⁻).

Some of the NO₂ molecules interact with interstitial oxygen anions forming NO₃⁻ ions as shown in equation 3.10. These NO₃⁻ ions may either stay inside the crystal lattice of Ta₂O₅ or in its vicinity to balance the overall charge of the composite molecule. Some of the NO₂ molecules get negatively charged accepting the released electrons (equation 3.12).

The oxygen vacancies in the sensor surface are filled in by the adsorbed oxygen species of the atmosphere. The adsorbed oxygen atoms, O_{ads}⁻ are accepted by NO₂ molecules as denoted by equation 3.13.



The CSA-PANi-Ta₂O₅ molecule undergoes interaction with NO₂ according to equations 3.11 and 3.12. When the thin film sensor comes in contact with a certain concentration of NO₂ gas, some of the gas molecules are adsorbed by the sensing surface. Being an oxidizing gas, NO₂ withdraws electrons, i.e., the negatively charged oxygen ions as shown in equations 3.11 and 3.12. This results in increase in the no. of hole carriers in the CSA-PANi-Ta₂O₅ layer improving its p-type conductivity. This is presented in equation 3.14.



The NO₂ gas exposure is intermittently turned off and on in cycles to examine the change in resistance of the sensing layer. This phenomenon is later illustrated in Fig. 3.19. The short-lived NO₂ bonded composite molecule, i.e. [(NO₃⁻)(NO₂⁻)(CSA-PANi-Ta₂O₅²⁺)] reverts back to its original state, viz., CSA-PANi-Ta₂O₅ when the gas is turned off (equation 3.14).

As the surface morphology suggests, PANi-Ta₂O₅ nanocomposite possesses well-formed spherical shapes. This kind of nanostructures carries larger contact area for the gas molecules and facilitates better adsorption by increasing no. of active sites on the sensor surface. Noble metals or their oxides when added to the sensing material, surface catalysis and surface adsorption sites are enhanced.

The gas sensing properties of the nanocomposite based sensors can further be improved by doping the polymer material with suitable organic acids such as CSA, DBSA (dodecyl

benzene sulphonic acid), pTSA (p-toluenesulphonic acid), tanninsulphonic acid, ligninsulphonic acid etc. This has been reported by several past works as discussed in the earlier chapter.

Polymers normally have low solubility and hence thin film based sensors suffer limitations in practical applications. The organic acids, mentioned above, have quite some strong Bronsted acid centers which can protonate polymers like PANi and induce more stability and greater solubility to its inflexible backbone chain [183]. Acid doping can also enhance the intrinsically low charge carrier density of the CPs and make them more conductive. It has been reported by several earlier studies that acid dopants can modify the structure, morphology, surface-to-volume ratio of the sensing material and increase nos. of active sites on the sensing surface thus facilitating gas sensing [59], [60], [184].

As explained earlier, the surface morphology of the CSA doped nanocomposites showed a visible impact of the doping effect of the organic acid. It exhibited clusters of highly aggregated globular structures (Fig. 2.19). The aggregation increased with the addition of higher percentages of CSA. These kind of nanostructures possess large surface area with abundant reactive sites [162] suitable for gas sensing.

3.4.2 Band gap theory

The gas sensing behaviour of the studied sample towards NO₂ gas can further be explained with the help of band-gap theory of PANi-Ta₂O₅ nanocomposite. Semiconducting metal oxides like SnO₂, ZnO, TiO₂, Ta₂O₅ can typically behave as n-type materials [185]. The addition of a metal oxide into the polymer matrix can induce change in surface morphology and result in heterojunctions. Due to different physical and chemical properties such as energy band structure, electron affinity, dielectric constant, lattice constant etc., heterojunctions with novel properties may emerge at the interface [185]. Many researchers worked on the synthesis of novel materials that resulted in the formation of heterojunctions and brought into additional advantages to gas sensing [186-190].

Ta₂O₅ is an n-type semiconductor with 3.8 eV energy band gap. PANi is a p-type semiconductor with 2.8 eV band gap. Ta₂O₅ interacts with PANi giving rise to p-n

heterojunction. A positively charged depletion layer is formed at the heterojunction due to possible inter-particle migration of electrons from Ta₂O₅ to PANi [191].

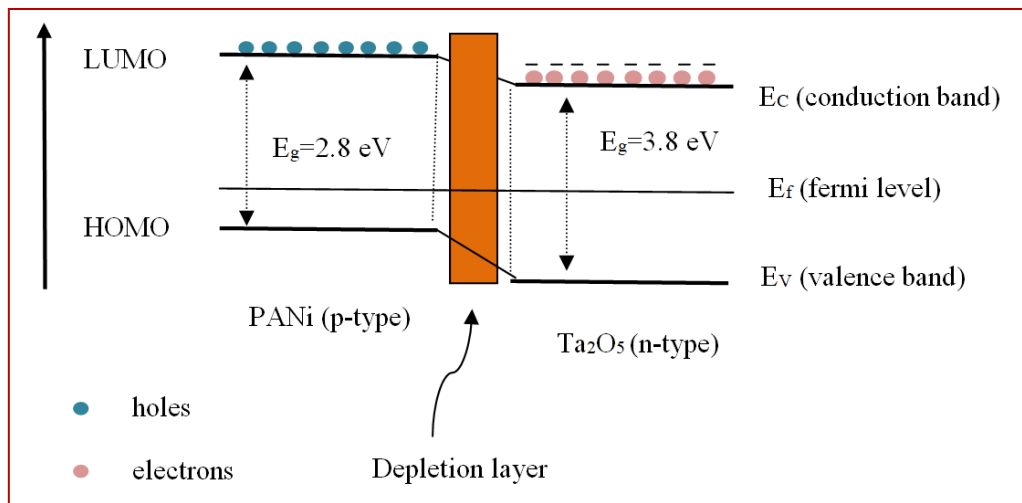
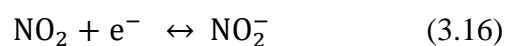
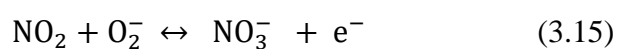


Fig. 3.16. possible formation of p-n heterostructure and energy band diagram of PANi-Ta₂O₅ nanocomposite.

While exposed to air, Ta₂O₅ could adsorb oxygen molecules on its surface, and these adsorbed molecules could then capture electrons from the conduction band of Ta₂O₅. The adsorbed oxygen molecules get transformed into different oxygen species (O₂⁻, O⁻, O²⁻) by ionizing (equations 3.1 through 3.4). This makes the depletion layer thicker, resulting in a narrower conduction channel and in increase in resistance [185]. The hole accumulation layer for conduction becomes narrower by the formation of hole depletion layer of the n-type Ta₂O₅. This offers an explanation of increase in resistance of the heterojunction.

When NO₂ gas is diffused, it withdraws the electrons from the sensing surface as shown in equations 3.15 and 3.16. This results in the decrease in free electron concentration in the conduction band of Ta₂O₅ and decrease the thickness of the positively charged depletion layer.



The formation of this depletion layer can be seen in Fig. 3.16. Charge transfer can smoothly take place between the LUMO of PANi and the conduction band of Ta₂O₅. This can enhance gas sensing performance [192]. When exposed to NO₂, PANi is protonated and the thickness of the depletion layer further diminishes. This would widen the conduction channel and the resistance of the p-n heterojunction decreases. The resistance change in the sensing material and the p-n heterojunction can change the potential barrier height at the interface and consequently the current increases across the junction [193], [194]. This aspect has an important contribution towards enhancing sensor response [191], [195].

Thus, according to the sensor response definition (table 3.1.a) for p-type semiconductor to electron-accepting gas, the formation of p-n heterojunction significantly improved the sensing response.

3.4.3 Scheme of formation of CSA doped PANi-Ta₂O₅ nanocomposite

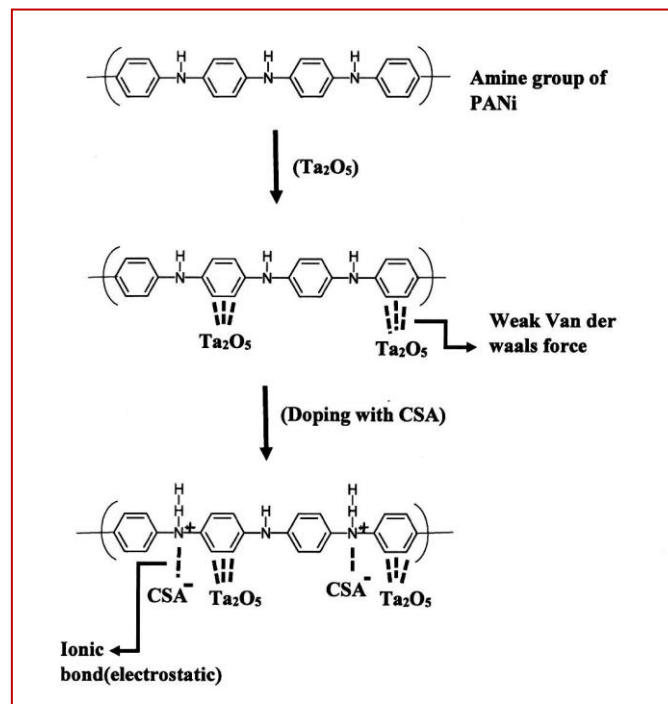


Fig.3.17. Schematic of formation of CSA doped PANi-Ta₂O₅ nanocomposite [75].

The influence of NO₂ on the conductivity of the PANi film is not simple. Conductivity of polyaniline depends on the degree of protonation as well as the degree of oxidization. NO₂ is an electron-accepting analyte which when comes in contact with the π -electron network of

polyaniline, captures electrons from the polymer matrix. When this occurs, the polymer becomes positively charged with holes. The charge carriers thus created give rise to increase in conductivity of the sensing film.

One important factor here is the role played by the oxygen atoms adsorbed at the sensing surface. This aspect was discussed in the earlier section. Fig. 3.17 illustrates the possible scheme for formation of CSA doped PANi-Ta₂O₅ molecule. It is possible that the Ta₂O₅ molecule is attached with the π cloud of the benzene ring of PANi through weaker secondary forces (intermolecular bonds) such as van der waals force [196]. Further, the doping of CSA results into protonation of amine (-NH) group of the PANi molecule. This can result into the formation of an ionic bond with electrostatic attraction between PANi and CSA molecule. The sulphonic acid group donates proton to the amine group of PANi, making the PANi backbone richer in positive charge.

3.4.4 Gas sensing characteristics

a) Sensor response (S)

The sensor response of the thin film samples of pure PANi, PANi-Ta₂O₅, PANi-Ta₂O₅-CSA20%, PANi- Ta₂O₅-CSA30% and PANi-Ta₂O₅-CSA40% was investigated at room temperature. In the present study, we have taken sensor response (S) [76], [67], [197] as shown in equation 3.17.

$$S = \frac{\Delta R}{R_a} \times 100\% \quad (3.17)$$

Here, where ΔR is the change in resistance of the sensor material in the presence of dry nitrogen gas (carrier gas) and that in the presence of a particular concentration of NO₂ plus the carrier gas. R_a is the resistance in the presence of the carrier gas only.

The resistance of the sensor was measured using Keithly 2100 6 ½ digital multimeter. The initial resistance of the PANi-Ta₂O₅ sample was recorded in hundreds of kilo ohms, while after doping with CSA the resistance decreased to a range of tens of kilo ohms. The lowest initial resistance for the 40% sample was recorded as 11.67 kilo ohms which reduced to about

2 kilo ohms upon exposure to the gas as shown in Fig. 3.18. The doping effect of CSA influenced the conductivity of the samples by facilitating the generation of polarons or bipolarons caused by electron delocalization effect [32].

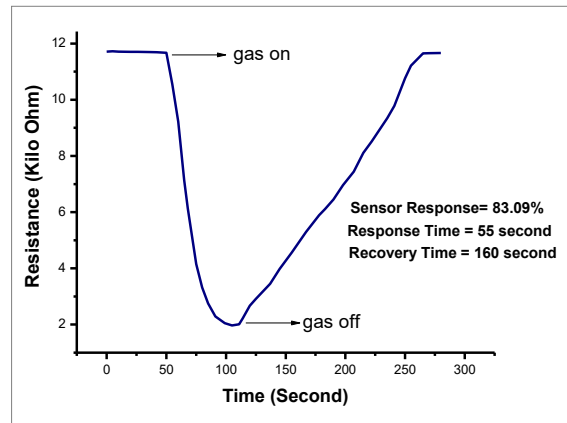


Fig. 3.18. Change in resistance of PANi-Ta₂O₅-CSA40% with respect to time towards 500 ppm of NO₂ gas [75].

The dependence of sensor response of the PANi samples on various concentrations of NO₂ gas can be studied from Fig. 3.19. As the thin film is exposed to the analyte gas, charge transfer takes place and more hole carriers are generated in the active layer according to scheme shown in Fig.3.17. This increases the p-type conductivity of the sensing material. With the increase in concentration of NO₂, conductivity of the sensing layer further increases. For all the five cases, the increase in sensor response was found linear till 500 ppm which turned slower after 700 ppm was reached. Finally, sensitivity almost reached saturation at 1000 ppm.

Pure PANi depicted a maximum sensor response of 43%, which enhanced to 57% upon addition of Ta₂O₅. The sensor response improved significantly with the increase in doping percentage of CSA in the nanocomposite. The increased agglomeration of the highly doped nanocomposite as evident from the SEM micrographs is one of the favorable morphologies for improving gas adsorption/desorption rate with improved nos. of sensing sites [59]. It is found that PANi-Ta₂O₅-CSA40% responded best with a highest response value of 88% at 1200 ppm. It is seen that pure PANi and PANi-Ta₂O₅ to be least sensitive with sensor

response less than 60%. Henceforth, in the subsequent sections the CSA doped samples are considered for examining the NO_2 gas sensing characteristics.

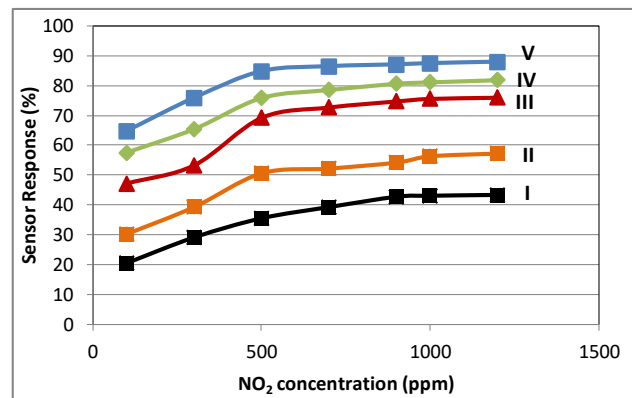


Fig. 3.19. Graphs of sensor response (%) versus NO_2 concentration (ppm) of I) pure PANi, II) PANi- Ta_2O_5 , III) PANi- Ta_2O_5 -CSA20%, IV) PANi- Ta_2O_5 -CSA30% and V) PANi- Ta_2O_5 -CSA40% [75].

b) Dynamic Response

Dynamic response transients of the CSA doped samples towards 500 ppm gas concentration are shown in Fig. 3.20. Each of the CSA doped thin film samples was exposed to 500 ppm NO_2 gas at room temperature for the time duration of 15 to 20 minutes.

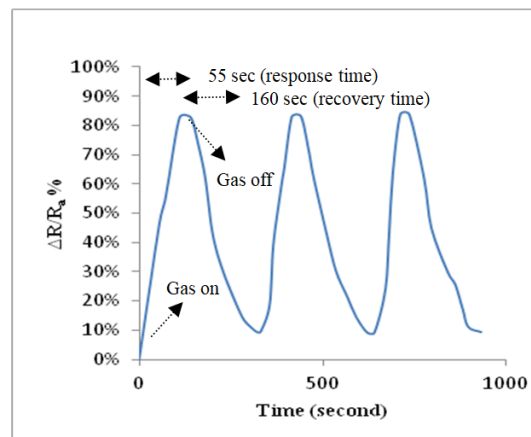


Fig. 3.20.a) Dynamic response plot of PANi- Ta_2O_5 -CSA40% to repetitive exposure to 500 ppm of NO_2 gas [75].

As the process initiates, each of the samples was kept in air for 50 seconds to stabilize and then exposed to the gas. Fig. 3.20.a shows the change in electrical resistance of the PANi- Ta_2O_5 -CSA40% sample with respect to time to 500 ppm of NO_2 . The graph showed a sharp

fall in resistance, i.e., increase in current after exposing the sample to the gas. The sample response reached a maximum value of 83.09% with a response time of 55 seconds. On removing the gas, resistance started to rise till it reached its original steady value with a recovery time of 160 seconds.

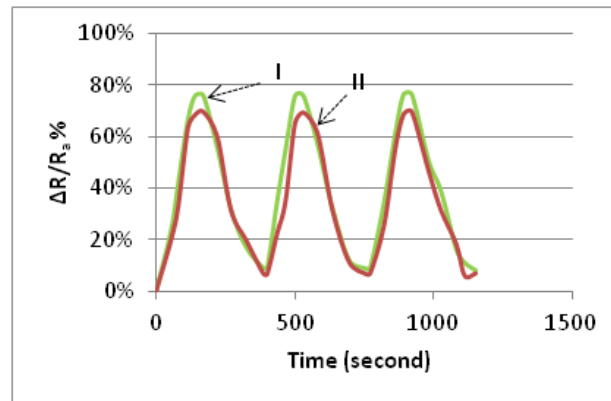


Fig. 3.20.b) Dynamic response plots of I) PANi-Ta₂O₅-CSA30% and II) PANi-Ta₂O₅-CSA20% to repetitive exposure of 500 ppm of NO₂ gas [75].

In Fig. 3.20, three cycles of repetitive exposure to 500 ppm of NO₂ are illustrated. In case of 40% CSA sample (Fig. 3.20.a), the first cycle depicted a response time of 55 seconds and recovery time as 160 seconds. It is observed that in all the cycles the maximum sensitivity attained 83% to 84%. All the three cycles showed good reproducibility. Dynamic response for 30% and 20% samples are shown in Fig. 3.20.b. The response of the nanocomposite at doping levels of 30% and 20% of CSA towards 500 ppm was obtained as high as 76% and 69% respectively. The response curves found reproducible. The response time for both the samples found longer as 85 seconds and 170 seconds respectively. Thus, it is observed that the PANi-Ta₂O₅-CSA40% performed much superior compared to the 30% and the 20% samples. This can be attributed for the enhanced interaction of the 40% nanocomposite material with the target gas which, in turn, would result from the formation of highly aggregated nanostructure (Fig. 2.19.e).

Existing studies established that this kind of morphology does possess a larger surface area with porous structure [198]. The reproducibility of the response curves can be caused due to the fact of adsorption and desorption of the analyte gas molecules at the sensing surface during the gas on-off cycles.

c) Response time and recovery time

The response time plots for different concentrations of NO₂ gas are shown in Fig. 3.21. The samples responded slowly for lower concentrations of the analyte gas. It took between 50 to 85 seconds for the response to reach 80% of the saturation value for the 40% and 30% samples at 500 ppm. The 40% sample showed the shortest response time of 55 seconds to 500 ppm gas. For all the three samples, the response time declines at a slower rate for lower concentrations (≤ 500 ppm) but faster as the concentration increases above 500 ppm and it almost kept steady beyond 1100 ppm. After a particular gas concentration, no more active sites remained in the surface to be filled to cause any significant effect.

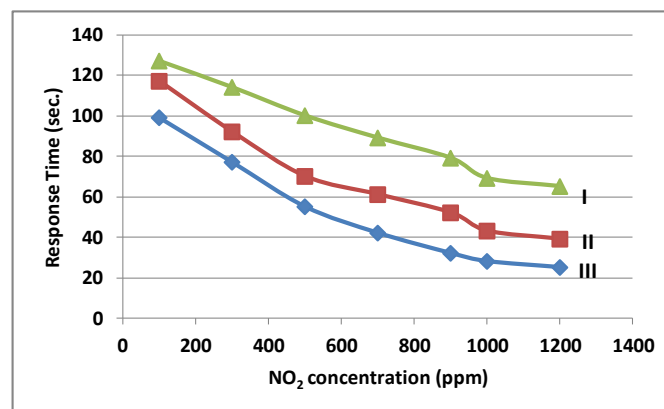


Fig. 3.21. Study of response time of I) PANi-Ta₂O₅-CSA20%, II) PANi-Ta₂O₅-CSA30% and III) PANi-Ta₂O₅-CSA40% to various concentrations of NO₂ gas [75].

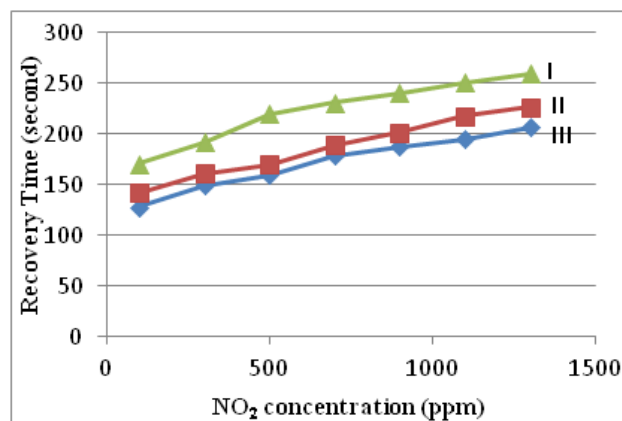


Fig. 3.22. Study of recovery time of I) PANi-Ta₂O₅-CSA20%, II) PANi-Ta₂O₅-CSA 30% and III) PANi-Ta₂O₅-CSA40% to varied concentrations of NO₂ gas [75].

The recovery time plots of the CSA doped samples are shown in Fig. 3.22. The recovery time towards various concentrations of NO₂ gas found to be relatively longer. For the 40% sample, recovery time is found as 128 seconds at 100 ppm NO₂ concentration. The recovery time is faster at lower concentrations but it gets longer as the gas concentration increases. All the three samples recovered at a faster rate till 700 ppm concentration. With high concentration of gas beyond 900 ppm, the samples took a longer time to restore back to its original steady-state resistance. For 20% and 30% samples, recovery time stood almost constant beyond 1000 ppm.

d) Study of humidity effect on sensor performance

Room temperature operated gas sensors often suffer from the the adverse effects of humidity of the surrounding atmosphere. It is a crucial task to examine the influence of moisture on the sensor performance.

In order to investigate the effect of humidity on the sensing performance, the sample (PANi-Ta₂O₅-CSA40% thin film) was exposed to three humid conditions with 38% RH, 57% RH and 65% RH respectively. For this experiment, the gas sensing setup shown in Fig. 3.14 was used with additional hardware. Sensor response of the sample was measured to check for any cross-sensitivity of the sensor towards varying levels of moisture in the surrounding atmosphere.

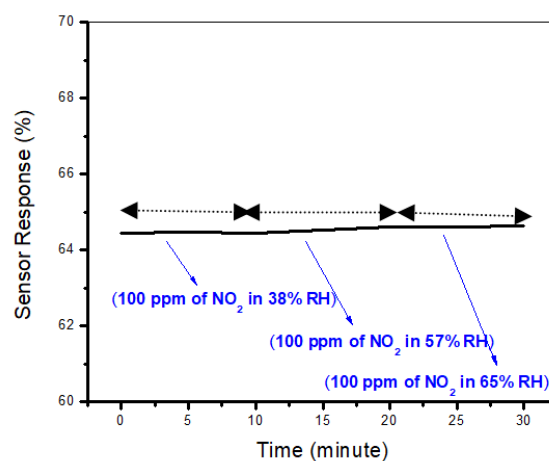


Fig. 3.23. Effect of relative humidity of the sensor utilizing PANi-Ta₂O₅-CSA40% [75].

A stream of humid air with different values of relative humidity (RH) was induced in the mixing gas chamber along with 100 ppm NO₂ gas. The sensor was exposed to a mixture of 100 ppm NO₂ and humid air with relative humidity of 38%, 57% and 65% respectively. The sensor response was recorded for three different humid levels, each test spanning for 10 minutes as shown in Fig. 3.23. An SH21 humidity sensor module was positioned next to the sensor device to examine in-situ the temperature and the humidity of the blended test gas flow and to get the sensor response data concurrently.

As evident from Fig. 3.23, the effect of different humidity content found very insignificant on the sensor response findings. The sensor response remained between 64% and 65% with negligible fluctuations under the three humid conditions of 38%, 57% and 65% RH with 100 ppm of NO₂ gas. Thus, the sensor displayed resistance to moisture at room temperature. This phenomenon may be explained as follows.

The water molecules present in the humid air possess very weak electron-withdrawing capacity. Their electron absorption will be overridden by the strong electron-withdrawing nature of NO₂ gas. Thus NO₂ gas played the most crucial part of the charge transfer process making the sensing surface least affected by the exposed humidity level.

e) Selectivity Study

Selectivity is an important index of sensing performance parameters. For the PANi-Ta₂O₅-CSA40% based sensor, selectivity to NO₂ gas was examined by exposing it to a host of potential interfering gases at room temperature. The sensor was exposed to 100 ppm of NO₂ gas and 500 ppm of each of the test gases. As depicted in Fig. 3.24, the sensor exhibited prominently high response to NO₂ gas, while it showed very small response to the test gases like NH₃, H₂S, CO and CO₂. This may be accounted for the following reason.

NO₂ is an electron-accepting molecule while NH₃ and H₂S are electron-donating molecules. So the latter two gases do not have the tendency to accept electron easily. Moreover, the electron-withdrawing capability of CO and CO₂ is less strong than that of NO₂ (due to the combined effect of three electronegative atoms in NO₂ and high electron deficiency of nitrogen atom) [199]. Therefore, NO₂ interacts more easily with the interstitial oxygen O_{i2}⁻ generated in the lattice of the sensing layer generating NO₃⁻ or NO₂⁻ (as explained in

equations 3.9 through 3.12). The sensor response towards the target gas directly correlates with the latter's interaction with the interstitial oxygen. Thus, it can be commented that the sensor under study exhibited considerably higher response towards NO₂ gas.

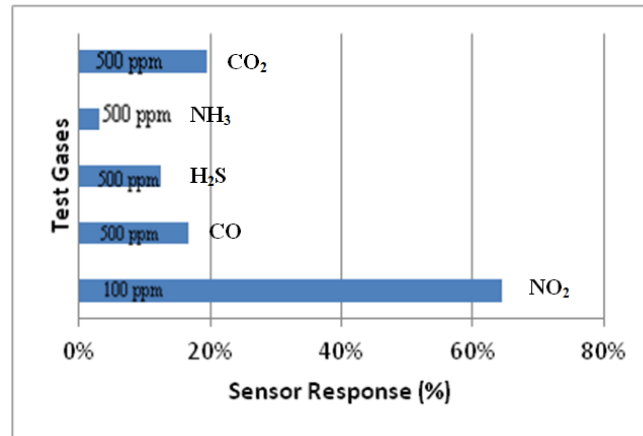


Fig. 3.24. Selectivity study of PANi-Ta₂O₅-CSA40% based sensor to 100 ppm NO₂ gas and 500 ppm of other test gases at room temperature [75].

a) Sensor Stability

The stability feature of the sensor towards 100 ppm concentration of NO₂ gas was observed for consecutive two months and is shown in Fig. 3.25.

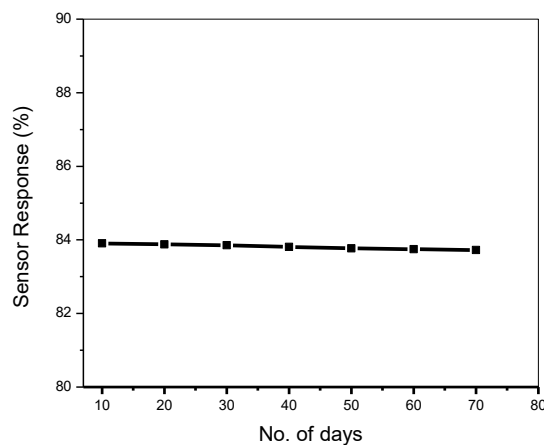


Fig.3.25. Stability study of the PANi-Ta₂O₅-CSA40% based sensor stored for 70 days at room temperature [75].

The PANi-Ta₂O₅-CSA40% based sample was stored at ambient condition for 70 days. After every 10 days, sensor response was measured by exposing the sample towards 100 ppm NO₂ gas. It was observed that the response showed slower decline towards the end of the

first 30 days. This may be accounted for obvious reasons of aging of the sensing film and continuous disappearance of the instable adsorption sites. It can be stated that the sensor showed a good stability over one month.

3.5 Chapter conclusions

This chapter reports the fabrication process and investigates the NO₂ gas sensing properties of PANi-Ta₂O₅-CSA based chemiresistive thin film device. The sensor response improved with the increase in doping percentage of CSA. The PANi-Ta₂O₅-CSA40% sample revealed the best results with the highest change in resistance on exposure to the gas. The sensor response reached as high as 83% towards 500 ppm gas. Sensor response escalated with the gas concentration owing to the emergence of fresh active sites thus facilitating more interactions between the analyte molecules and the sensing layer. The response time of the studied material was found to be reasonably faster, but a relatively slower recovery time was revealed by all the three CSA doped samples.

The PANi-Ta₂O₅-CSA40% based sensor showed high selectivity towards NO₂ gas. The sensor response retained its sensor response almost constant atleast over one month. The sensor device was least influenced by the surrounding humidity conditions, operating reliably at room temperature.
